J. Fluid Mech. (2019), *vol.* 871, R2, doi:10.1017/jfm.2019.309

JFM RAPIDS
journals.cambridge.org/rapids

Non-universal scaling transition of momentum cascade in wall turbulence

Xi Chen[1,†], **Fazle Hussain**[1,†] **and Zhen-Su She**[2,†]

[1]Department of Mechanical Engineering, Texas Tech University, TX 79409, USA

[2]State Key Laboratory for Turbulence and Complex Systems and Department of Mechanics, College of Engineering, Peking University, Beijing 100871, China

(Received 18 March 2019; revised 9 April 2019; accepted 10 April 2019; first published online 24 May 2019)

As a counterpart of energy cascade, turbulent momentum cascade (TMC) in the wall-normal direction is important for understanding wall turbulence. Here, we report an analytic prediction of non-universal Reynolds number (Re_τ) scaling transition of the maximum TMC located at y_p. We show that in viscous units, y_p^+ (and $1 + \overline{u'v'}_p^+$) displays a scaling transition from $Re_\tau^{3/7}$ ($Re_\tau^{-6/7}$) to $Re_\tau^{3/5}$ ($Re_\tau^{-3/5}$) in turbulent boundary layer, in sharp contrast to that from $Re_\tau^{1/3}$ ($Re_\tau^{-2/3}$) to $Re_\tau^{1/2}$ ($Re_\tau^{-1/2}$) in a channel/pipe, countering the prevailing view of a single universal near-wall scaling. This scaling transition reflects different near-wall motions in the buffer layer for small Re_τ and log layer for large Re_τ, with the non-universality being ascribed to the presence/absence of mean wall-normal velocity V. Our predictions are validated by a large set of data, and a probable flow state with a full coupling between momentum and energy cascades beyond a critical Re_τ is envisaged.

Key words: turbulence theory

1. Introduction

Energy cascade is one of the most important concepts in turbulence (Frisch 1995; Sreenivasan 1999; Jimenez 2012; Vassilicos 2015). It is featured by a nearly constant energy flux across multiscales of turbulent eddies, described by the following energy budget equation (Frisch 1995):

$$\partial_t E(k) + \partial_k \Pi(k) = \mathcal{F}(k) + 2\nu k^2 E(k). \tag{1.1}$$

Here, $E(k)$ is the energy spectrum, $\Pi(k)$ is the energy transfer rate, $\mathcal{F}(k)$ is the energy injection by forcing and $2\nu k^2 E(k)$ is the dissipation rate. The celebrated

† Email addresses for correspondence: chenxi97@outlook.com, fazle.hussain@ttu.edu, she@pku.edu.cn

inertial range is defined by a quasi-equilibrium state (i.e. $\partial_k \Pi(k) \approx 0$) where the energy flux is constant across scales (the so-called energy cascade) until dissipated at the smallest scales, and the spectrum E displays the famous $-5/3$ Kolmogorov scaling. Characteristic lengths such as integral scale (L), Taylor microscale (λ) and Kolmogorov scale (η) are fundamental metrics to quantify energy cascade of homogeneous turbulence (Frisch 1995; Sreenivasan 1999).

On the other hand, for canonical wall turbulence, there seems to exist a counterpart of energy cascade, i.e. turbulent momentum cascade (TMC), which was proposed as early as the 1970s in the monograph by Tennekes & Lumley (1972) under the concept of spatial inertial sublayer. The TMC is a relatively new concept but has received much attention recently (Jimenez 2012; G. Falkovich 2017, talk given at Frontiers in Turbulence: KRS70 at Denver Symposium, Colorado, USA; Yang & Lozano-Durán 2017). Consider the streamwise mean momentum equation (in a channel for example):

$$\partial_t U(y) + \partial_y \overline{u'v'}(y) = \mathcal{P}(y) + \nu \partial \partial_y U(y), \tag{1.2}$$

where $\partial_y \overline{u'v'}$ is the momentum transfer rate along the wall-normal (y) direction (overline indicates ensemble average in time and in the streamwise x and spanwise z directions for channel and pipe (CP) flows, or in the spanwise direction for turbulent boundary layer (TBL) flows; $'$ indicates fluctuation – that is, $u' = u - U$ and $v' = v - V$); $\mathcal{P} = -\partial_x \bar{p}/\rho$ is the momentum input by pressure gradient and $\nu \partial \partial_y U$ is the viscous shear stress. The inertial range of TMC can be similarly defined as the spatial domain subject to $\partial_y \overline{u'v'}(y) \approx 0$, around a characteristic location y_p where $\partial_y \overline{u'v'}(y) = 0$. Thus, y_p is the location of the exact quasi-equilibrium state for the momentum cascade, indicating the middle of the inertial sublayer. Note that y_p is a special location which demarcates the viscous inner scaling and inertial-dominated outer scaling regions, as examined carefully by Wei *et al.* (2005) and Klewicki (2013). This inner region boundary is previously known as the critical layer (Sreenivasan 1988). Here, y_p can be considered as a scale analogy to λ, since $\eta \ll \lambda \ll L$ while $\nu/u_\tau \ll y_p \ll \delta$ (ν/u_τ is the viscous scale with u_τ the friction velocity; δ is the half-height of channel, pipe radius or boundary layer thickness δ_{99}). Moreover, at y_p, Reynolds shear stress $-\overline{u'v'}$ is maximum and the mean shear $S = \mathrm{d}U/\mathrm{d}y$ shows a -1 power law in y at large Re (hence the celebrated von Kármán log law of U), analogous to the $-5/3$ spectrum in k.

Nevertheless, almost 50 years since Tennekes and Lumley's proposal, TMC has not yet been quantified clearly, and two fundamental questions remain unanswered: how the location y_p varies with the friction Reynolds number Re_τ, and how fast the TMC approaches the asymptotic momentum flux u_τ^2 with increasing Re_τ. Although a $Re_\tau^{1/2}$ scaling of y_p for CP at asymptotically high Re_τ has been known (Sreenivasan 1988) and is now widely used in the literature (Klewicki 2013; Chin *et al.* 2014; Lee & Moser 2015; Ahn, Lee & Sung 2017), no analysis of y_p has been performed for TBL, let alone the maximum momentum flux (or cascade), which requires a deeper insight. As emphasized by Falkovich (Frontiers in Turbulence: KRS70 at Denver Symposium, Colorado, USA (2017)), momentum cascade is a critical concept of fundamental interest for the study of wall turbulence; it involves not only scale-dependent contributions to Reynolds shear stress (Kawata & Alfredsson 2018), but also spatial inhomogeneity due to mean shear. Recent theoretical efforts with some success on CP flows include, for example, Goldenfeld (2006), who studied scaling theories for friction coefficients in smooth and rough pipes, and L'vov, Procaccia &

Rudenko (2008) for the U scaling. However, none of these studies has addressed TBL, due to the lack of understanding of the wall-normal momentum transfer by V (whose influence on the scaling of U and $\overline{-u'v'}$ was not realized before). Here, a unified treatment of CP and TBL is achieved, with a discovery of non-universal scaling transition.

Recently, we obtained an accurate description of mean velocity and turbulence intensities in CP based on the dilation symmetry of several stress length functions (She, Chen & Hussain 2017; Chen, Hussain & She 2018). This theory has been applied to describe other flows (for example, supersonic and hypersonic flows (She *et al.* 2018), and flow over a rough wall (She *et al.* 2012)), and is applied here to analyse the momentum cascade in CP and TBL. Specifically, we show here that there exists a scaling transition for increasing Re_τ, which is a direct consequence of the multilayer structure in CP and TBL; its interest is similar to the Re_λ-scaling transition of homogeneous turbulence from Gaussian to anomalous flow states found by Yakhot & Donzis (2017). At large Re, we show that y_p^+ in TBL follows a $Re_\tau^{3/5}$ scaling, in contrast to $Re_\tau^{1/2}$ in CP, countering the prevailing view of a single universal $1/2$ scaling. If the proposed new scalings are accepted, many earlier proposals (for example, see Wei *et al.* (2005), Wei (2018) and references therein) regarding $y_p^+ \propto Re_\tau^{1/2}$, which is suggested in the literature as the onset location of the log law, need to be revised.

2. Results

As illustrated in figure 1, y_p in TBL is notably larger than that in CP at a common $Re_\tau \approx 1000$, and our prediction implies that this critical layer of y_p in TBL becomes increasingly thicker than that of CP with increasing Re_τ. This has a practical significance, as y_p can be an engineering-relevant quantity: in the drag control of wall flows, a recent study by Yao, Chen & Hussain (2018) shows that the optimal controlling parameter, i.e. the height of large-scale swirls excited by actuators, follows the Re_τ scaling of y_p.

Recall the near-wall motion described by viscous units $y^+ = yu_\tau/\nu$, and the outer inertial-dominated flow region by y/δ. Sreenivasan (1988) proposed the $Re_\tau^{1/2}$ scaling of y_p^+ for CP at high Re_τ, validated by many others later (Klewicki 2013; Chin *et al.* 2014; Lee & Moser 2015; Ahn *et al.* 2017). This can be derived as follows. Integrating (1.2) with respect to y^+ yields

$$W^+ = \tau^+ - S^+ \tag{2.1}$$

(where the total stress $\tau^+ = 1 - y^+/Re_\tau$); further provided with the log law:

$$S^+ \approx 1/(\kappa y^+), \tag{2.2}$$

it readily yields

$$y_{p-CP}^+ = (Re_\tau/\kappa)^{1/2} \approx 1.5 Re_\tau^{1/2} \tag{2.3}$$

by setting $\mathrm{d}W^+/\mathrm{d}y^+ = 0$ (κ is the von Kármán constant with its value taken around 0.45; see She *et al.* (2017) and Chen *et al.* (2018)). However, equation (2.3) is not accurate for CP at moderate Re_τ (Ahn *et al.* 2017), as seen in figure 2, showing a clear scaling transition.

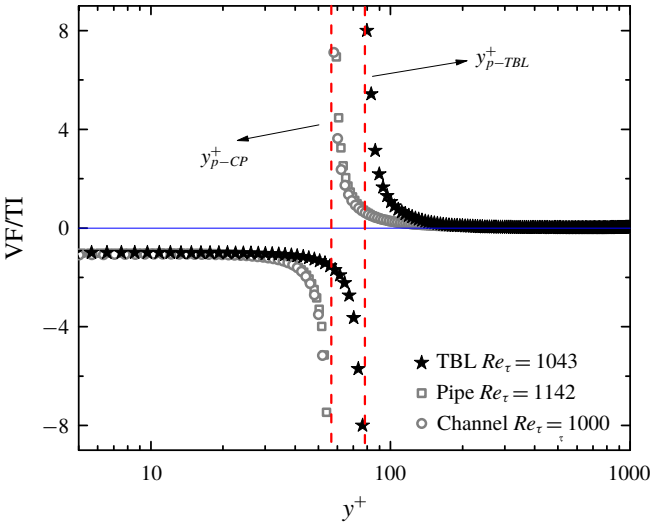

FIGURE 1. Ratio between the viscous shear force VF ($\partial S^+/\partial y^+$) and turbulent inertial TI ($\partial W^+/\partial y^+$) showing the inner and outer flow regions demarcated by $y^+ = y_p^+$ where $\partial W^+/\partial y^+ = 0$. Here, $W^+ = -\overline{u'v'}^+$ and $S^+ = \partial U^+/\partial y^+$. Symbols are DNS data: stars from Schlatter *et al.* (2010); squares from Wu & Moin (2008); circles from Lee & Moser (2015).

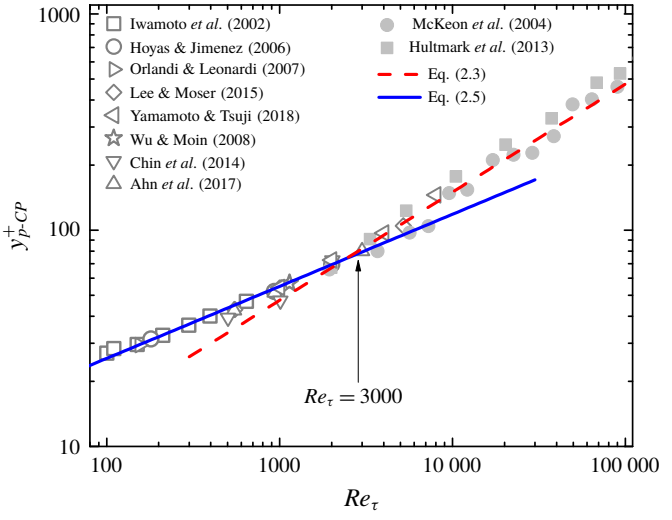

FIGURE 2. Scaling transition for the critical layer (y_p^+) of momentum cascade. Solid line denotes (2.5) for low *Re* and dashed line denotes (2.3) for high *Re*. Open symbols, DNS channel and pipe; solid symbols, experimental pipe.

This discrepancy of the classical scaling analysis is now well resolved here, through a specification of the buffer layer beneath the log layer, yielding a scaling transition towards lower *Re*. Specifically, the viscous buffer layer extends from $y_{sub}^+ \approx 9.7$ to $y_{buf}^+ \approx 41$, and we introduce a stress length ($\ell^+ = \sqrt{W^+}/S^+$) which takes the following

analytic form (She *et al.* 2017; Chen *et al.* 2018):

$$\ell^+ \approx (\kappa y_{sub}^{+1/2}/y_{buf}^+)y^{+3/2} \quad \text{for } y^+ \ll y_{sub}^+; \tag{2.4a}$$

$$\ell^+ \approx (\kappa/y_{buf}^+)y^{+2} \quad \text{for } y_{sub}^+ \lesssim y^+ \lesssim y_{buf}^+; \tag{2.4b}$$

$$\ell^+ \approx \kappa y^+ \quad \text{for } y_{buf}^+ \ll y^+ \ll Re_\tau. \tag{2.4c}$$

This allows us to examine the scaling of y_p for small Re_τ, such that $y_p^+ \lesssim y_{buf}^+$.

Substituting the approximation $S^+ \approx 1/\ell^+$ with (2.4*c*) into (2.1), we obtain (2.3) for high Re_τ; but for small Re_τ, with (2.4*b*), we obtain:

$$y_{p-CP}^+ = Re_\tau^{1/3}(2y_{buf}^+/\kappa)^{1/3} \approx 5.7Re_\tau^{1/3}. \tag{2.5}$$

The existence of the buffer layer y^{+2} scaling is the key to the present discovered scaling transition; this scaling arises from a local quasi-balance between the residue viscous effect ε and turbulent production SW, as follows. Introduce a shear eddy length: $\ell_\nu = (W/S)^{3/4}\varepsilon^{-1/4}$; expansion analysis shows that $\ell_\nu \propto y^2$ as $y \to 0$ (She *et al.* 2017). Note that $\ell^+ = \ell_\nu^+ \Theta^{1/4}$, where $\Theta = \varepsilon/(SW)$. As shown in She *et al.* (2017), in the sublayer, $\Theta \ll 1$ and $\ell_\nu^+ \ll \ell^+$, and near-wall motion is dominated by random fluctuations; Taylor expansion results in (2.4*a*). However, in the buffer layer, Θ reaches a maximum of order unity (due to dominant effect of coherent motion); then, ℓ^+ follows the scaling of ℓ_ν^+, which is (2.4*b*). In the log layer where $\Theta \approx 1$, $\ell \approx \ell_\nu \propto y$ from homogeneous dilation symmetry (Chen *et al.* 2018), which is (2.4*c*).

The realization of a buffer layer leads to a physical interpretation for the above scaling transition. Note that cascade is normally considered to result from the multiscale dynamics of turbulence (Frisch 1995). For the energy cascade, many studies have shown that it is caused by vortex stretching (for example, Goto 2009); for the momentum cascade, according to Jimenez (2012) and Yang & Lozano-Durán (2017), it is carried out by a hierarchy of multiscale wall-attached eddies, which transfer momentum towards the wall until it is drained by the viscous effect. In Jimenez (2018), it is shown that the logarithmic eddies (or vortex clusters) scale as y, which yield a scaling as predicted by (2.4*c*); moreover, the buffer layer eddies are viewed as in an autonomous cycle having smaller sizes but with a higher Corrsin shear parameter, in accordance with (2.4*b*), which indicates a smaller ℓ and hence a larger S. Thus, approaching the wall from log to buffer layers, eddies with different spatial organizations, not surprisingly, would dictate different cascade processes.

We now validate the predicted scaling transition by empirical data. Note that unlike for DNS data, it is quite inaccurate to determine y_p^+ from the experimentally measured $\overline{u'v'}$ profile (for example, with large scatter); thus, an alternative way to determine y_p^+ is needed. Taking a y^+-derivative of (2.1) at $y^+ = y_p^+$ yields

$$-Re_\tau \, \mathrm{d}S^+/\mathrm{d}y^+(y_p^+) = 1, \tag{2.6}$$

which presents an equivalent way to find y_p^+ from $S^+(y^+) = \partial U^+/\partial y^+$. It is more accurate since the twice y^+-derivative of $U^+(y^+)$ can be obtained more reliably. For the Princeton SuperPipe (McKeon *et al.* 2004; Hultmark *et al.* 2013), as $\overline{u'v'}$ data are absent, Chin *et al.* (2014) and Ahn *et al.* (2017) determine y_p^+ in this way.

Figure 2 shows that (2.5) agrees well with data at smaller Re_τ, which, together with (2.3), indicates that the $Re_\tau^{0.372}$ scaling by data fitting over the Re_τ range 500–5200 in Ahn *et al.* (2017) is perhaps a misinterpretation. Furthermore, we predict

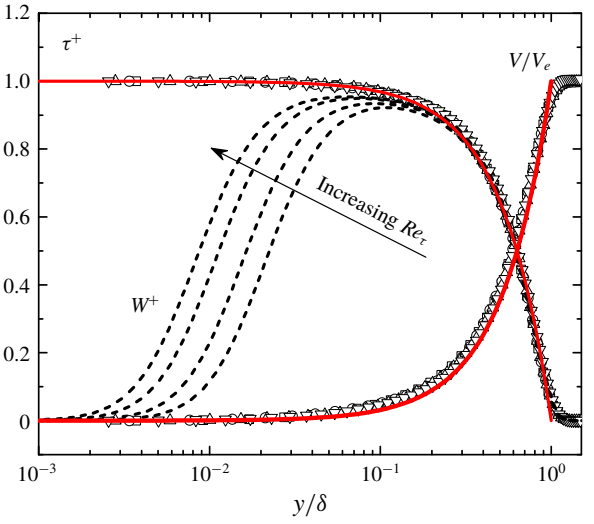

FIGURE 3. DNS profiles (Schlatter *et al.* 2010) of total stress τ^+ (symbols), mean wall-normal velocity V/V_e (symbols) and mean momentum flux (Reynolds shear stress) $W^+ = -\overline{u'v'}^+$ (dashed lines) in TBL. Profiles of τ^+ and V/V_e at four different cases $Re_\tau = 492$, 671, 974 and 1271 collapse. Solid lines indicate our theories: equation (2.7) for V and (2.8) for τ^+.

that the scaling transition from $Re_\tau^{1/3}$ to $Re_\tau^{1/2}$ takes place around $Re_\tau^{(crit)} = 4\kappa y_{buf}^{+2} \approx 3000$ for CP, by equating (2.5) with (2.3). Evidently, the $Re_\tau^{1/3}$ scaling in figure 2 in turn supports the intermediate scaling (2.4*b*) in the buffer layer. Whilst the scaling transition in CP has been shown in Chen *et al.* (2018), here we include more data sets (for Re_τ covering three decades) to provide compelling evidence of scaling transition. More importantly, the theme of the current paper is to reveal and demonstrate, under the same analysis, the non-universal scaling transition among CP (internal) and TBL (external) flows, as we discuss below.

Applying the above analysis to TBL, a new element arises – that is, a small but finite mean wall-normal velocity V. The small V changes the U profile only slightly, but leads to its non-trivial streamwise development, and a different total stress, i.e. $\tau^+ = 1 - \int_0^{y^+} (U^+(\partial V^+/\partial y') - V^+(\partial U^+/\partial y'))\,\mathrm{d}y'$. For determining V, we consider the mean kinetic energy equation of V, in which the dissipation term (that is, $\epsilon_V = \nu(\partial V/\partial y)^2$) can be specified by a dimensional analysis using ν, δ and free-stream wall-normal velocity V_e, yielding $\epsilon_V = (\nu V_e^2/\delta^2)\Omega(y/\delta)$. The self-similar function Ω satisfies $\Omega(0) = 0$, which suggests a simple linear approximation: $\Omega = \omega_1 y/\delta$, and then, $\epsilon_V = \omega_1(\nu V_e^2/\delta^2)(y/\delta)$. Using the definition of ϵ_V and integrating it with respect to y, one obtains

$$V/V_e = (2\sqrt{\omega_1}/3)(y/\delta)^{3/2} = (y/\delta)^{3/2}, \tag{2.7}$$

where $\omega_1 = (3/2)^2 = 9/4$ due to $V(0) = 0$ and $V(\delta) = V_e$. Figure 3 shows that (2.7) agrees closely with DNS data, which thus well describes the data collapse found by Wei & Klewicki (2016).

Based on (2.7), τ^+ in TBL is obtained:

$$\tau^+ \approx 1 - (y/\delta)^{3/2} = 1 - (y^+/Re_\tau)^{3/2}. \tag{2.8}$$

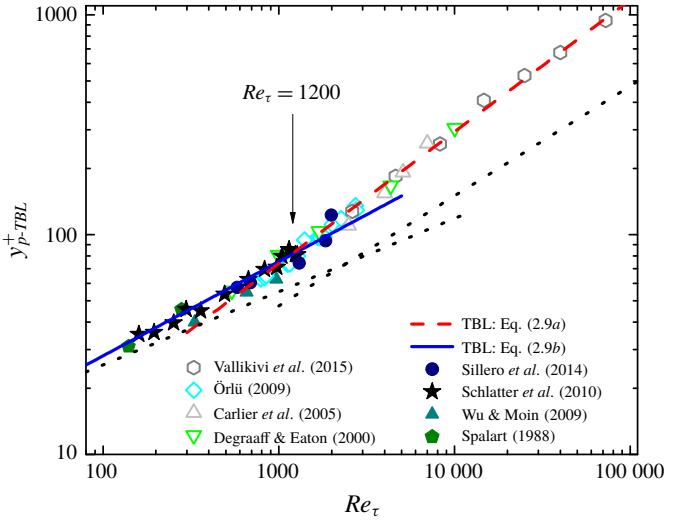

FIGURE 4. The same plot as figure 2 but for TBL. Solid symbols, DNS; open symbols, experiments. Note that the open symbols of experiments are measured by using (2.10) – agreeing well with solid symbols of DNS data in the overlapped Re_τ range (from 500 to 2000). For comparison, two dotted lines for CP are included, which show much smaller y_p^+ for high Re.

To see this, we first denote $U^+ \propto (y^+)^\xi$, where according to the log law (2.2), $\xi - 1 \approx -1$ or $\xi \approx 0$ (also see Barenblatt (1993), where $\xi \propto 1/\ln Re$). Then, substituting $U^+ \propto (y^+)^\xi$ and $V^+ \propto (y^+)^{3/2}$ of (2.7) into $\tau^+ = 1 - \int_0^{y^+} (U^+(\partial V^+/\partial y') - V^+(\partial U^+/\partial y'))\,\mathrm{d}y'$ yields $1 - \tau^+ \propto (y^+)^{3/2+\xi}$. As $\xi \approx 0$, $1 - \tau^+ \approx \tau_0 y^{+3/2}$. Moreover, as $\tau^+ = 0$ at $y^+ = \delta^+$ (or $y^+ = Re_\tau$), $\tau_0 = Re_\tau^{-3/2}$, and thus (2.8). Compared to $1 - \tau^+ = y^+/Re_\tau$ in CP, $1 - \tau^+$ in TBL is higher at the same y location due to V. This explains earlier observations in Degraaff & Eaton (2000), well supported by DNS data in figure 3.

Completing the previous analysis of y_p^+ using (2.8) yields

$$y^+_{p-TBL} = Re_\tau^{3/5}(2/3\kappa)^{2/5} \approx 1.1 Re_\tau^{3/5} \tag{2.9a}$$

for large Re_τ, and

$$y^+_{p-TBL} = Re_\tau^{3/7}(4y^+_{buf}/3\kappa)^{2/7} \approx 3.9 Re_\tau^{3/7} \tag{2.9b}$$

for small Re_τ. The relation defining y_p^+ from $\mathrm{d}S^+/\mathrm{d}y^+$ for TBL takes the following form:

$$-(Re_\tau^{3/2}/\sqrt{y^+})\,\mathrm{d}S^+/\mathrm{d}y^+(y_p^+) = 3/2, \tag{2.10}$$

in sharp contrast to (2.6) for CP. Again, equating (2.9b) and (2.9a), the scaling transition occurs around $Re_\tau = 2(9\kappa^2 y^{+5}_{buf})^{1/3} \approx 1200$.

Figure 4 shows the good agreement between the prediction (2.9) and data. Note that y^+_{p-TBL} between DNS data (Spalart 1988; Wu & Moin 2009; Sillero, Jimnez & Moser 2014) – by pinpointing the maximum of the W^+ profile directly – and experimental data (Degraaff & Eaton 2000; Carlier & Stanislas 2005; Örlü 2009; Vallikivi, Ganapathisubramani & Smits 2015) – by using (2.10) – agree well with

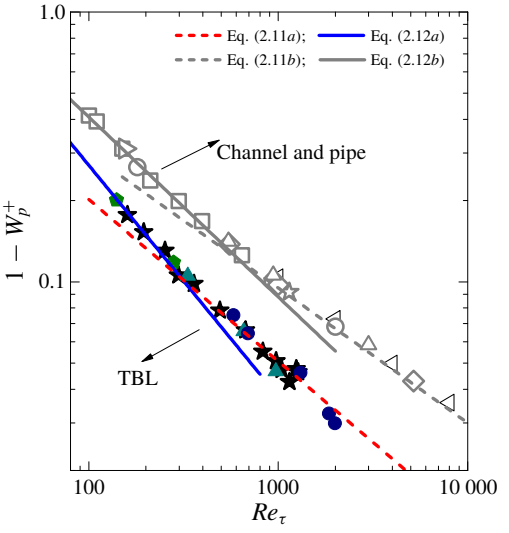

FIGURE 5. Scaling transition for the maximum momentum flux ($1 - W_p^+ = 1 + \overline{u'v'}_p^+$). Note that solid symbols are DNS TBL data, the same as in figure 4, while open symbols are DNS CP data, the same as in figure 2.

each other in the overlapped Re_τ range, hence supporting the validity of (2.10). Moreover, we have checked that $W^+ \approx 1 - (y^+/Re_\tau)^{3/2}$ agrees closely with the available high-Re_τ experimental W^+ profile in the outer flow region; thus (2.8) and hence (2.10) seem robust. Incidentally, a $Re_\theta^{0.63}$ scaling was reported for TBL based on fitting of experimental data (Fernholz & Finleyt 1996), which is quite close to our (2.9a) (as $Re_\theta/Re_\tau \sim O(1)$; see Chen & She (2016), Monkewitz, Chauhan & Nagib (2007)). However, those TBL experimental data have too much scatter, and hence are not included here.

The non-universal scaling transition is also reflected in the maximum momentum flux $W_p^+ (= -\overline{u'v'}_p^+)$, which is obtained by substituting y_p^+ in (2.1). For large Re_τ, using (2.9a) for TBL and (2.3) for CP, respectively, we have

$$1 - W_{p-TBL}^+ = (5/2)(2/3\kappa)^{3/5} Re_\tau^{-3/5} \approx 3.2 Re_\tau^{-3/5}, \tag{2.11a}$$

$$1 - W_{p-CP}^+ = (2/\sqrt{\kappa}) Re_\tau^{-1/2} \approx 3.0 Re_\tau^{-1/2}; \tag{2.11b}$$

for small Re_τ, using (2.9b) and (2.5), we have

$$1 - W_{p-TBL}^+ = (7/4)(4y_{buf}^+/3\kappa)^{3/7} Re_\tau^{-6/7} \approx 13.7 Re_\tau^{-6/7}, \tag{2.12a}$$

$$1 - W_{p-CP}^+ = 3(y_{buf}^+/4\kappa)^{1/3} Re_\tau^{-2/3} \approx 8.5 Re_\tau^{-2/3}. \tag{2.12b}$$

Figure 5 shows $1 - W_p^+$ displaying a distinguished scaling transition, well described by (2.11) and (2.12). Note that $1 - W_p^+$ and y_p^+ have different dependences on Re_τ, and their transitions are continuous and not sharp. As a result, the transition values of Re_τ estimated by the simply crossing of low- and high-Re_τ scalings are different. For example, equating (2.11a) with (2.12a) we obtain a crossover Re_τ for $1 - W_p^+$ in TBL (i.e. $Re_\tau \approx 300$) – much smaller than 1200 for the transition of y_p^+. That is why

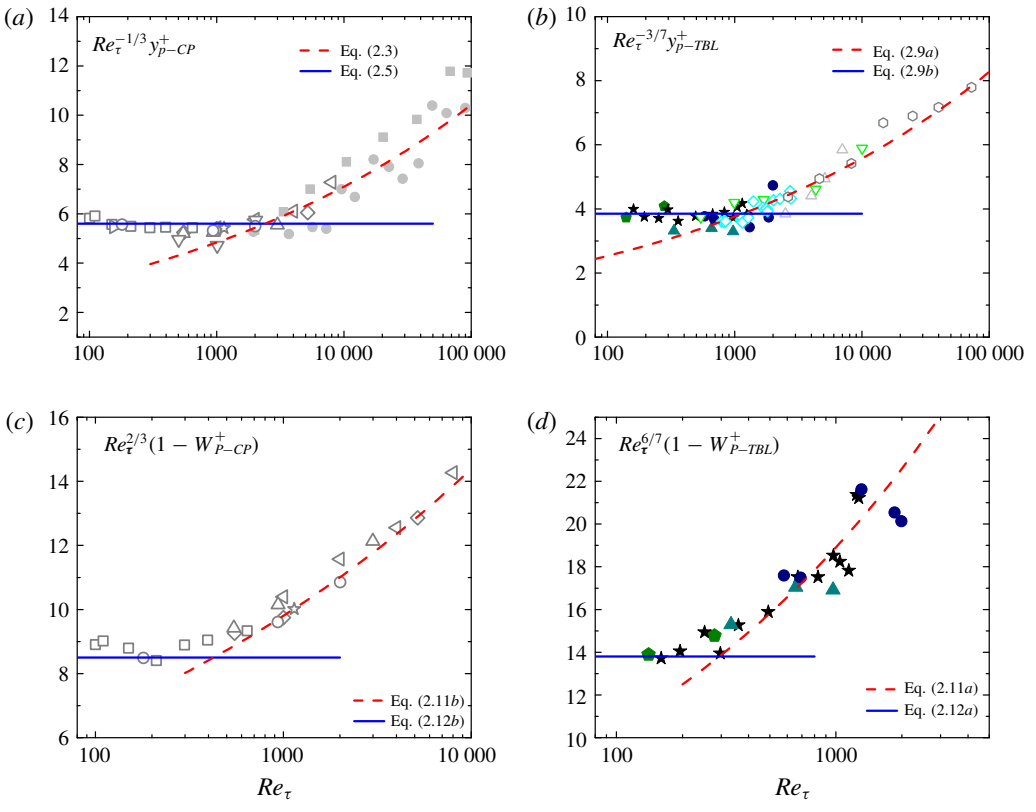

FIGURE 6. Compensated plots of y_p^+ scaling for channel and pipe flows (a), and for TBL flows (b). Compensated plots of $1 - W_p^+$ scaling for channel and pipe flows (c), and for TBL flows (d). Lines are scaling predictions; symbols are data – the same as in figure 2 (for channel and pipe) and figure 4 (for TBL).

for the same DNS data sets, scaling transitions are observed for $1 - W_p^+$ in figure 5, but not for y_p^+ in figure 4.

To better display the scaling transition, we show in figure 6 the compensated plots of both y_p^+ and $1 - W_p^+$. The plateaus in figure 6(a,b) justify the small-Re scaling $Re_\tau^{1/3}$ for CP and $Re_\tau^{3/7}$ for TBL, respectively; data departing from the plateaus indicate the scaling transition with increasing Re_τ. For example, for channel flows, most DNS data follow the $Re_\tau^{1/3}$ scaling; however, DNS data at $Re_\tau = 4000$ (Yamamoto & Tsuji 2018), 5200 (Lee & Moser 2015) and 8000 (Yamamoto & Tsuji 2018) agree better with (2.3) than with (2.5), hence clearly displaying the predicted scaling transition. Moreover, figure 6(c,d) show the transition in $1 - W_p^+$, where most DNS data are in the large-scaling regimes. It is unknown why the scaling transition for $1 - W_p^+$ is less sharp and occurs earlier than that for y_p^+, possibly due to $1 - W_p^+$ being a subleading-order behaviour of the momentum cascade (the leading-order behaviour is $W^+ \approx 1$ as $Re \to \infty$), which varies mildly but sensitively with increasing Re. A further examination on the vorticity transport of W^+ (Chin *et al.* 2014) is perhaps helpful to answer this question. Note the deviation from (2.11a) for the two largest Re data points in figure 6(d), which may suggest a new scaling trend but may also be caused

by insufficiently large simulation domains – an issue to clarify when high-quality data at large Re are available.

According to the DNS data trend and our predictions in figure 5, $1 - W_p^+ < 0.03$ for CP at $Re_\tau = 10^4$ and $1 - W_p^+ < 0.01$ at $Re_\tau = 10^5$; the deviation from unity is even smaller for TBL (i.e. $1 - W_p^+ < 0.01$ at $Re_\tau = 10^4$ and $1 - W_p^+ < 0.003$ at $Re_\tau = 10^5$). These small deviations are far beyond the experimental resolutions, and hence we use DNS data to validate our predictions of $1 - W_p^+$. It is clear from figures 5 and 6(*c*,*d*) that the predicted large-Re scalings are well supported by both CP and TBL DNS data; while for small Re, there are only a few data points in these figures, showing mild deviations from our large-Re predictions, but they all follow closely our scaling predictions for small Re. One can of course fit the solid symbols in figure 5 (i.e. $1 - W_p^+$ of TBL) by a single power law (for example, $6.2Re_\tau^{-0.7}$), but then one cannot explain these fitting parameters. Moreover, the fitting may be another data misinterpretation, as there is a scaling transition according to our theory.

Finally, let us envisage the existence of an asymptotic flow state for CP and TBL by the probable full coupling between energy and momentum cascades. While the energy cascade is more developed in the bulk flow region ($y^+ > y_Q^+$ with $y_Q^+ \sim 150$–200) where production quasi-balances dissipation, the momentum cascade is centred at $y^+ = y_p^+$, which is smaller than y_Q^+ at moderate Re_τ but would overtake y_Q^+ as Re_τ increases. Therefore, equating $y_p^+ = y_Q^+$, we obtain a critical Re_τ indicating the onset of co-existence of two cascades in the bulk flow. It was speculated (Chen *et al.* 2015) that at this state the energy cascade will be modified, leading to anomalous energy dissipation. Taking $y_Q^+ \approx 150$ for CP (Vincenti *et al.* 2013) yields $Re_\tau^{(c)} = \kappa y_Q^{+2} \approx 10\,100$, which interestingly matches $Re_\tau \approx 10\,481$ for the emergence of an outer $\overline{u'u'}$ peak in the Princeton SuperPipe (Hultmark *et al.* 2013). For TBL, $y_Q^+ \approx 200$ (Schlatter *et al.* 2010), using y_p^+ in (2.9) we obtain another critical $Re_\tau^{(c)} \approx 5500$, very close to $Re_\tau \approx 6400$ where the outer $\overline{u'u'}$ peak in TBL is observed (Vincenti *et al.* 2013). This apparent link to the emergence of the $\overline{u'u'}$ outer peak is intriguing, which implies a possible asymptotic flow regime for Reynolds number larger than $Re_\tau^{(c)}$.

3. Conclusion

In this paper, we establish a non-universal Re-scaling transition for both the peak location and the magnitude of Reynolds shear stress (momentum cascade). Particularly, at large Re, we show that y_p^+ in TBL follows a $Re_\tau^{3/5}$ scaling, in contrast to $Re_\tau^{1/2}$ in CP – countering the prevailing view of a single universal $Re_\tau^{1/2}$ scaling. If the proposed new scalings are accepted, earlier proposals suggesting $y_p^+ \propto Re_\tau^{1/2}$ need to be revised. Notwithstanding the scatter in the experimental data, our predicted y_p^+ and $1 - W_p^+$ both agree with all DNS data of CP and TBL flows; hence supporting the non-universal scaling transition for the three canonical wall flows.

References

AHN, J., LEE, J. & SUNG, H. J. 2017 Contribution of large-scale motions to the Reynolds shear stress in turbulent pipe flows. *Intl J. Heat Fluid Flow* **66**, 209–216.

BARENBLATT, G. I. 1993 Scaling laws for fully developed turbulent shear flows. Part 1. Basic hypotheses and analysis. *J. Fluid Mech.* **248**, 513–520.

CARLIER, J. & STANISLAS, M. 2005 Experimental study of eddy structures in a turbulent boundary layer using particle image velocimetry. *J. Fluid Mech.* **535**, 143–188.

CHEN, X., HUSSAIN, F. & SHE, Z. S. 2018 Quantifying wall turbulence via a symmetry approach. Part 2. Reynolds stresses. *J. Fluid Mech.* **850**, 401–438.

CHEN, X. & SHE, Z. S. 2016 Analytic prediction for planar turbulent boundary layers. *Sci. China Phys. Mech. Astron.* **59** (11), 114711.

CHEN, X., WEI, B. B., HUSSAIN, F. & SHE, Z. S. 2015 Anomalous dissipation and kinetic-energy distribution in pipes at very high Reynolds numbers. *Phys. Rev.* E **93**, 011102(R).

CHIN, C., PHILIP, J., KLEWICKI, J., OOI, A. & MARUSIC, I. 2014 Reynolds-number-dependent turbulent inertia and onset of log region in pipe flows. *J. Fluid Mech.* **757**, 747–769.

DEGRAAFF, D. B. & EATON, J. K. 2000 Reynolds-number scaling of the flat plate turbulent boundary layer. *J. Fluid Mech.* **422**, 319–346.

FERNHOLZ, H. H. & FINLEYT, P. J. 1996 The incompressible zero-pressure-gradient turbulent boundary layer: an assessment of the data. *Prog. Aerospace* **32**, 245–311.

FRISCH, U. 1995 *Turbulence: The Legacy of A. N. Kolmogorov*. Cambridge University Press.

GOLDENFELD, N. 2006 Roughness-induced critical phenomena in a turbulent flow. *Phys. Rev. Lett.* **96**, 044503.

GOTO, S. 2009 Turbulent energy cascade caused by vortex stretching. In *Advances in Turbulence XII* (ed. B. Eckhardt), Springer Proceedings in Physics, vol. 132. Springer.

HOYAS, S. & JIMENEZ, J. 2006 Scaling of the velocity fluctuations in turbulent channels up to $Re_\tau = 2003$. *Phys. Fluids* **18** (1), 011702.

HULTMARK, M., VALLIKIVI, M., BAILEY, S. C. C. & SMITS, A. J. 2013 Logarithmic scaling of turbulence in smooth- and rough-wall pipe flow. *J. Fluid Mech.* **728**, 376–395.

IWAMOTO, K., SUZUKI, Y. & KASAGI, N. 2002 Database of fully developed channel flow. *Tech. Rep.* ILR-0201.

JIMENEZ, J. 2012 Cascades in wall-bounded turbulence. *Annu. Rev. Fluid Mech.* **44**, 27–45.

JIMENEZ, J. 2018 Coherent structures in wall-bounded turbulence. *J. Fluid Mech.* **842**, P1.

KAWATA, T. & ALFREDSSON, P. H. 2018 Inverse interscale transport of the Reynolds shear stress in plane Couette turbulence. *Phys. Rev. Lett.* **120**, 244501.

KLEWICKI, J. C. 2013 Self-similar mean dynamics in turbulent wall flows. *J. Fluid Mech.* **718**, 596–621.

LEE, M. & MOSER, R. D. 2015 Direct numerical simulation of turbulent channel flow up to $Re_\tau \approx 5200$. *J. Fluid Mech.* **774**, 395–415.

L'VOV, V. S., PROCACCIA, I. & RUDENKO, O. 2008 Universal model of finite Reynolds number turbulent flow in channels and pipes. *Phys. Rev. Lett.* **100** (5), 054504.

MCKEON, B. J., LI, J., JIANG, W., MORRISON, J. F. & SMITS, A. J. 2004 Further observations on the mean velocity distribution in fully developed pipe flow. *J. Fluid Mech.* **501**, 135–147.

MONKEWITZ, P. A., CHAUHAN, K. A. & NAGIB, H. M. 2007 Self-consistent high-Reynolds-number asymptotics for zero-pressure-gradient turbulent boundary layers. *Phys. Fluids* **19** (11), 115101.

ORLANDI, P. & LEONARDI, S. 2007 *Tech. Rep.* WT-071016-URS-1. WALLTURB project.

ÖRLÜ, R. 2009 Experimental studies in jet flows and zero pressure-gradient turbulent boundary layers. PhD thesis, KTH Royal Institute of Technology, Stockholm.

SCHLATTER, P., LI, Q., BRETHOUWER, G., JOHANSSON, A. V. & HENNINGSON, D. S. 2010 Simulations of spatially evolving turbulent boundary layers up to $Re_\theta = 4300$. *Intl J. Heat Fluid Flow* **31** (3), 251–261.

SHE, Z. S., CHEN, X. & HUSSAIN, F. 2017 Quantifying wall turbulence via a symmetry approach: a Lie group theory. *J. Fluid Mech.* **827**, 322–356.

SHE, Z. S., WU, Y., CHEN, X. & HUSSAIN, F. 2012 A multi-state description of roughness effects in turbulent pipe flow. *New J. Phys.* **14** (9), 093054.

SHE, Z. S., ZOU, H.-Y., XIAO, M.-J., CHEN, X. & HUSSAIN, F. 2018 Prediction of compressible turbulent boundary layer via a symmetry-based length model. *J. Fluid Mech.* **857**, 449–468.

SILLERO, J. A., JIMNEZ, J. & MOSER, R. D. 2014 Two-point statistics for turbulent boundary layers and channels at Reynolds numbers up to $\delta^+ = 2000$. *Phys. Fluids* **26** (10), 105109.

SPALART, P. R. 1988 Direct simulation of a turbulent boundary layer up to $re_\theta = 1410$. *J. Fluid Mech.* **187**, 61–98.

SREENIVASAN, K. R. 1988 *Turbulence Management and Relaminarization*. Springer.

SREENIVASAN, K. R. 1999 Fluid turbulence. *Rev. Mod. Phys.* **71**, S383–S395.

TENNEKES, H. & LUMLEY, J. L. 1972 *A First Course in Turbulence*. Cambridge University Press.

VALLIKIVI, M., GANAPATHISUBRAMANI, B. & SMITS, A. J. 2015 Spectral scaling in boundary layers and pipes at very high Reynolds numbers. *J. Fluid Mech.* **771**, 303–326.

VASSILICOS, J. C. 2015 Dissipation in turbulent flows. *Annu. Rev. Fluid Mech.* **47** (1), 95–114.

VINCENTI, P., KLEWICKI, J., MORRILL-WINTER, C., WHITE, C. M. & WOSNIK, M. 2013 Streamwise velocity statistics in turbulent boundary layers that spatially develop to high Reynolds number. *Exp Fluids* **54**, 1629.

WEI, T. 2018 Integral properties of turbulent-kinetic-energy production and dissipation in turbulent wall-bounded flows. *J. Fluid Mech.* **854**, 449–473.

WEI, T., FIFE, P., KLEWICKI, J. & MCMURTRY, P. 2005 Properties of the mean momentum balance in turbulent boundary layer, pipe and channel flows. *J. Fluid Mech.* **522**, 303–327.

WEI, T. & KLEWICKI, J. 2016 Scaling properties of the mean wall-normal velocity in zero-pressure-gradient boundary layers. *Phys. Rev. Fluids* **1**, 082401(R).

WU, X. H. & MOIN, P. 2008 Direct numerical simulation on the mean velocity characteristics in turbulent pipe flow. *J. Fluid Mech.* **608**, 5–41.

WU, X. H. & MOIN, P. 2009 Direct numerical simulation of turbulence in a nominally zero-pressure-gradient flat-plate boundary layer. *J. Fluid Mech.* **630**, 5–41.

YAKHOT, V. & DONZIS, D. 2017 Emergence of multiscaling in a random-force stirred fluid. *Phys. Rev. Lett.* **119**, 044501.

YAMAMOTO, Y. & TSUJI, Y. 2018 Numerical evidence of logarithmic regions in channel flow at $Re_\tau = 8000$. *Phys. Rev. Fluids* **3**, 012602.

YANG, X. I. A. & LOZANO-DURÁN, A. 2017 A multifractal model for the momentum transfer process in wall-bounded flows. *J. Fluid Mech.* **824**, R2.

YAO, J., CHEN, X. & HUSSAIN, F. 2018 Drag control in wall-bounded turbulent flows via spanwise opposed wall-jet forcing. *J. Fluid Mech.* **852**, 678–709.